Observation of Inner Electron Ionization from Radial Rydberg Wave Packets in Two-Electron Atoms

H. Maeda, W. Li, and T. F. Gallagher

Department of Physics, University of Virginia, Charlottesville, Virginia 22901

(Received 7 August 2000; revised manuscript received 12 October 2000)

We have observed multiphoton ionization of the $5s$ core electron from a $5snd$ radial Rydberg wave packet of Sr atoms using a short optical pulse. When the outer nd electron is at its outer turning point the inner $5s$ electron is removed from the atom, and the outer electron is left in a Sr^+ Rydberg state, but when the outer electron is at the inner turning point this does not occur. Analysis of the final Sr^+ Rydberg states shows that the two electrons interact as the inner electron leaves, so that the outer electron is not simply projected onto the Sr^+ Rydberg states.

PACS numbers: 32.80.Rm, 31.70.Hq, 42.50.Hz

While the response of "single-electron" atoms to intense laser pulses is now reasonably well understood, the response of "many-electron" atoms is not, because of the interactions among the electrons [1]. In view of this complication, it is hardly a surprise that He and the alkaline earth atoms, with two valence electrons, have been investigated intensely [2]. However, even in these, the simplest many-electron atoms, the physics is not completely clear.

One of the simplest forms of multiphoton ionization in a two-electron atom is inner electron ionization (IEI), observed almost a decade ago by Stapelfeldt *et al.* [3] and Jones and Bucksbaum [4]. They observed that when an atom in a bound Ba $6snd$ Rydberg state is exposed to an intense laser pulse of duration less than the Kepler orbit time of the nd electron, $\tau_K = 2\pi n^3$, the inner $6s$ electron can be removed from the atom while the outer nd electron remains bound in a Rydberg state of Ba^+ of the same orbital size as the initial $6snd$ state. Here n is the principal quantum number. These observations are consistent with the following simple picture. For a laser pulse shorter than τ_K, in some of the $6snd$ atoms the outer nd electron does not come near the core during the laser pulse and cannot absorb a photon. However, the Ba^+ $6s$ ionic core absorbs several photons and is ionized, and the inner $6s$ electron leaves the atom in a time short compared to the orbit time τ_K of the outer electron. Thus, in these atoms the outer electron is projected from the initial Ba nd Rydberg state onto Ba^+ Rydberg states. In contrast, for a laser pulse longer than τ_K, in all of the atoms the outer electron comes near the core during the laser pulse and can absorb a laser photon, or the two electrons can easily exchange energy if the inner electron absorbs a photon. In either case, the outer electron is ejected and not left in a Ba^+ Rydberg state, hence the observed dependence of IEI on the length of the laser pulse relative to τ_K.

While this picture is appealing, recent experimental results of Tate and Gallagher [5] and Rosen *et al.* [6] are inconsistent with the notion of a projection of the outer electron from the Ba Rydberg state onto the Ba^+ Rydberg states and suggest that the interaction between the electrons during IEI plays an important role.

Although the explanation of IEI given above is based on a time-domain picture, all of the experiments to date have been done by exposing atoms in Rydberg eigenstates to the intense laser pulse. If, instead, a radial wave packet, in which the Rydberg electron oscillates between its inner and outer turning points, is exposed to an intense short pulse we expect to observe IEI when the Rydberg electron is at its outer turning point but not at its inner turning point. Furthermore, if the outer Rydberg electron is projected from the neutral wave packet, the final ion Rydberg states depend in a simple way on the position of the Rydberg electron when the laser pulse arrives. Here we report the first observations of IEI starting from a Sr $5snd$ Rydberg wave packet. The experiments confirm the basic picture but indicate that interaction between the two electrons during IEI is indeed important.

Figure 1 depicts the basic idea of preparing and ionizing the Sr $5snd$ Rydberg wave packet. Ground state $5s^2\,{}^1S_0$ Sr atoms in an atomic beam are exposed to a sequence of three laser pulses at a 20-Hz repetition rate. The atoms are excited to the $5s6p\,{}^1P_1$ state by a 293-nm pulse obtained by frequency doubling a 5-ns-long, 586-nm dye laser pulse. The $5s6p$ atoms are then excited to a coherent superposition of $5sns$ and $5snd$ states by a 200-fs, 854-nm pulse from an amplified titanium:sapphire laser. Since the dominant excitation is to the $5snd$ states, the resulting wave packet is essentially a $5snd$ wave packet with an average principal quantum number, $\bar{n}$, which can be varied over the range $26 \leq \bar{n} \leq 35$.

After a variable time delay the atoms are exposed to a 200-fs, 427-nm pulse obtained by doubling the 854-nm pulse. It is nearly resonant with the Sr^+ $5s \rightarrow 5p$ transition at 422 nm and efficiently ionizes Sr^+ $5s$ ions by the four-photon process shown in Fig. 1. The 427-nm light is produced by angle tuning a 0.5-mm-long BBO crystal, and the angle is set so as to maximize the IEI signal. The 427-nm light is tightly focused by a 50-cm focal length lens, giving a peak intensity of 8×10^{12} W/cm^2. The 854-nm beam, whose energy is 150 μJ per pulse, is focused with a 2-m focal length lens and is limited to a 40 cm^{-1} bandwidth by a polarizer.

 0031-9007/00/85(24)/5078(4)$15.00

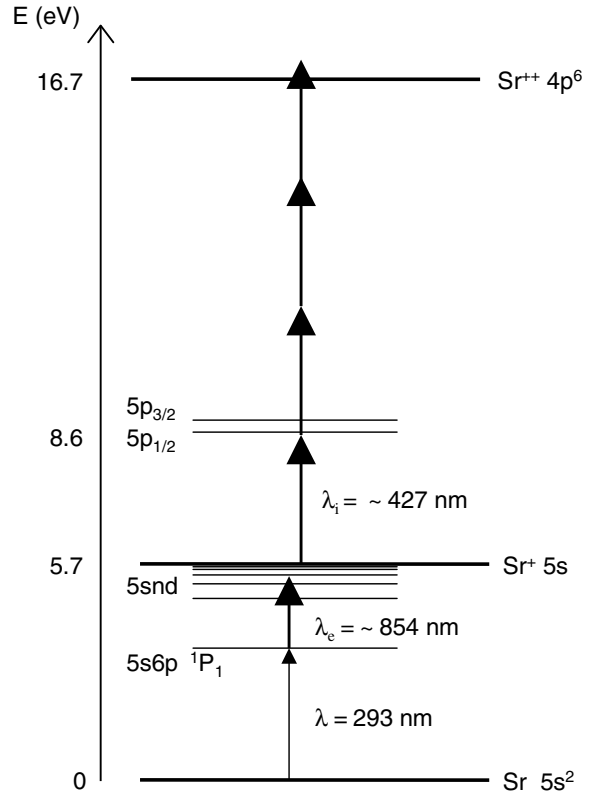

FIG. 1. Strontium energy level diagram, showing the excitation of the Sr 5*snd* wave packet by the first two laser pulses at 293 and 854 nm. After time delay t, the third pulse at 427 nm ionizes the Sr^+ 5*s* electron. Absorption of four photons by Sr^+ 5*s* ions produces a free electron of 0.6 eV kinetic energy.

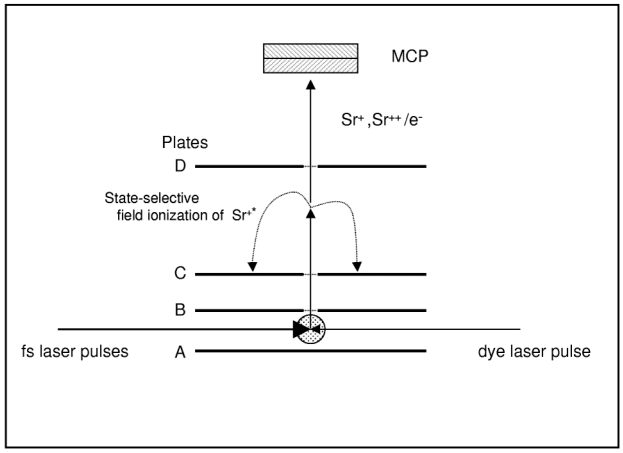

FIG. 2. Diagram of the interaction region of the apparatus. The ions from field ionization of Sr^* and Sr^{+*}, together with Sr^+ and Sr^{++} ions, follow the path of the two solid arrows. In the case where we detect electrons, the ions follow the lower solid arrow and the electrons from field ionization of Sr^{+*} follow the upper solid arrow, while Sr^{+*}, Sr^+, and Sr^{++} follow the dotted curved arrows.

As shown by Fig. 2, the three laser beams are collinear and intersect the Sr effusive atomic beam at a right angle between a pair of plates, A and B, separated by 3 mm. Approximately 100 ns after the laser pulses, an adjustable (0–9 kV) positive pulsed voltage of 1-μs rise time is applied to plate A, while plate B is grounded, field ionizing both the Sr 5*snd* Rydberg wave packet and highly excited Sr^{+*} ions. The field pushes all ions produced through a mesh in the upper plate toward a dual microchannel plate (MCP) detector. Plates C and D are grounded or held at an appropriate negative voltage. We detect the time-resolved signals from Sr Rydberg states, Sr^+, Sr^+ Rydberg states, and Sr^{++}, which we denote by Sr^*, Sr^+, Sr^{+*}, and Sr^{++}, respectively. We typically set a gate on the signal of interest and scan the time delay between the second and third laser pulses.

Figure 3 shows typical IEI signals obtained by varying the time delay, starting with a Sr 5*snd* wave packet which has nearly 80% of its population in four states. The time delay t is expressed in terms of the classical orbit time τ_K, where $\tau_K = 2.9$ ps for $\bar{n} = 26.8$. Figure 3(a) was obtained by setting a gate on the Sr^{+*} signal. It is evident that the IEI signal of Fig. 3(a) undergoes several oscillations at period τ_K, and that the maxima occur at $t = \frac{1}{2}\tau_K$, $\frac{3}{2}\tau_K$, and $\frac{5}{2}\tau_K$, while the minima occur at $t = 0$, τ_K, and $2\tau_K$. In other words, the probability of IEI is a maximum when the *nd* electron is at its outer turning point and a minimum when it is at its inner turning point, as expected. It is also evident that the oscillations are damped and their period modified after several clear oscillations, due to spreading of the radial wave packet. However, the signal becomes very clear again at about $t = 9\tau_K$, close to the predicted time of the first full revival of the wave packet, $8.9\tau_K$ [7].

By using the known excitation probabilities of the Sr 5*snd* states in the wave packet, it is straightforward to construct $\Psi(t)$, the time-dependent wave function of the wave packet, using Coulomb wave functions. With this wave function we have calculated the photoionization probability $|\langle \epsilon f|r|\Psi(t)\rangle|^2$ of the wave packet as shown in Fig. 3(b), which should be inversely related to the IEI probability. As shown, it is in good agreement with the data of Fig. 3(a). We have also calculated $|\langle \Psi(t)|1/r^2|\Psi(t)\rangle|$, which gives a reasonable estimate of the time-dependent interaction between the two electrons, and the result is indistinguishable, apart from a scale factor, from the result shown in Fig. 3(b). Consequently, on the basis of this measurement we are unable to differentiate between these two probable causes of the failure of IEI, and can only say that it does not occur if the outer electron is near the core. In Fig. 3(c) we show the multiphoton ionization signal of Sr^{++} which is taken simultaneously with the Sr^{+*} signal of Fig. 3(a) using a second gate. Since the Sr^{++} signal is usually much larger than that of Sr^{+*}, the characteristic modulation at τ_K is less clear than in the Sr^{+*} signal. However, careful comparison of these two signals shows a 180° out-of-phase relationship between them, as expected from early observations of IEI from Ba Rydberg states [4,5].

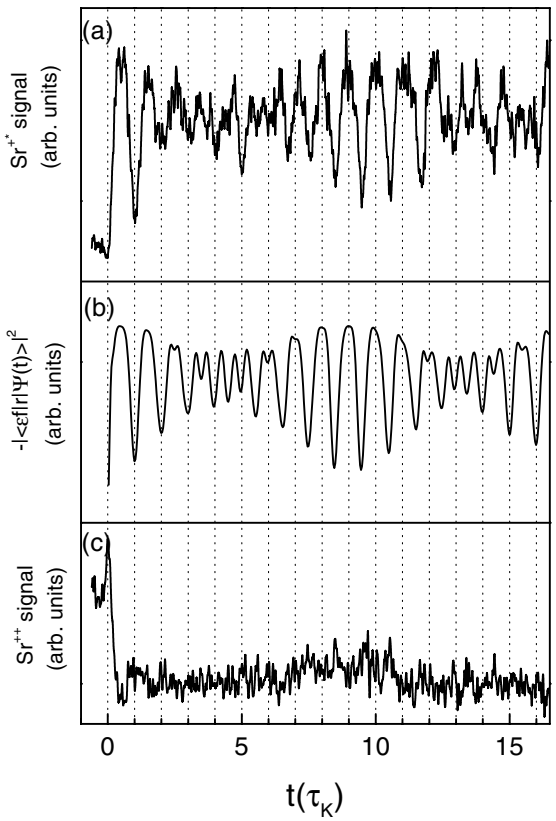

FIG. 3. The IEI signal from the Sr $5snl$ wave packet at $\bar{n} = 26.8$ plotted against the delay t; (a) the Sr^{+*} field-ionization signal, (b) the calculated $-|\langle \epsilon f|r|\Psi(t)\rangle|^2$, and (c) the Sr^{++} ion signal.

The IEI signal from wave packets of $26 \leq \bar{n} \leq 35$ shows, in all cases, the characteristic modulation at τ_K. Unexpectedly, the IEI signal still exhibits clear modulation even at the end of a delay scan longer than 220 ps, up to five full revivals in the case of $\bar{n} = 30.8$. The fact that five revivals are visible might be attributed to the fact that this method does not require phase coherence between two laser pulses, in contrast to bound-state interferometry [8].

By using the technique of Vrijen and Noordam [9], we can detect electrons from the field ionized Sr^{+*} instead of the ions, as shown in Fig. 2. After the ions are ejected from the interaction region between plates A and B with a small (10 V) voltage pulse and have reached the region between plates C and D, we apply a 1-μs rise time, negative 8–9 kV voltage ramp to plate C to field ionize Sr^{+*} and eject the electrons to the detector. Plate D is held at -70 V to suppress background electrons.

As expected, the total Sr^{+*} field-ionization electron signal is nearly identical to the Sr^{+*} ion signal of Fig. 3(a). More interesting, because different Rydberg states are ionized at different fields [10], the time-resolved electron signal can be converted to a final Sr^{+*} state distribution, from which we can obtain insight into the electron correlation during IEI. It is instructive to consider first what happens if the inner electron is suddenly ejected, in the simple one-dimensional classical model. When the inner electron is ejected at time t, it passes the outer electron at orbital radius $R(t)$, and the outer electron is projected onto the Sr^+ Rydberg states. In the projection the outer electron keeps the same position, momentum, and kinetic energy. Before interaction, the outer electron has energy $W_I = -1/2n_I^2$. We use atomic units if units are not explicitly given. At the interaction point $R(t)$, the kinetic energy of the outer electron is $W_I + 1/R(t)$, and it remains constant as the electron is projected onto the Sr^{++} potential. Thus, the total energy W_{II} of the Sr^+ Rydberg electron is $W_{II} = W_I - 1/R(t)$. Using the fact that $W_{II} = -2/n_{II}^2$, and using n_I and n_{II} for the principal quantum numbers of the initial Sr and final Sr^+ Rydberg states, we can write n_{II} in terms of n_I and $R(t)$ as,

$$n_{II} = \sqrt{\frac{2R(t)}{1 + R(t)/2n_I^2}}. \tag{1}$$

If the inner electron overtakes the outer electron at its outer turning point, $R = -1/W_I$, and Eq. (1) yields $n_{II} = \sqrt{2}\, n_I$. On the other hand, if the inner electron overtakes the outer electron between the inner and outer turning point, $R < -1/W_I$ and $n_{II} < \sqrt{2}\, n_I$.

In Fig. 4 we show the time-resolved Sr^{+*} field-ionization electron signals from different times in the evolution of a wave packet of $\bar{n} = 30.8$. The traces shown are obtained by subtracting a background signal from the observed signals. We could not detect signals lower than $n_{II} \simeq 30$ due to a large background signal there. The sequence of scans starts with the outer nd electron at its outer turning point, $t = \frac{1}{2}\tau_K$, moving into its inner turning point at $t = \tau_K$, and returning to its outer turning point at $t = \frac{3}{2}\tau_K$. The horizontal scale of Fig. 4 is labeled assuming that ionization of Sr^{+*} occurs adiabatically, at the field $F_{ad} = Z^3/16n_{II}^4$, where $Z = 2$ is the charge of the Sr^{++} core. We have used several combinations of polarizations of the two fs laser pulses, with no discernible effect on the final-state distribution.

If the outer electron is projected from Sr to Sr^+ Rydberg states, Eq. (1) predicts a single peak which moves with time t as shown by the locations of the arrows in Fig. 4. In contrast, the experimental final-state distributions are double peaked and only move slightly to lower n_{II} as t is increased from $t = \frac{1}{2}\tau_K$ to τ_K. It is clear from Fig. 4 that the electron is not simply projected onto ionic Sr^+ Rydberg states.

The doublet structure of Fig. 4 is surprising. It might be due to two different field-ionization paths, i.e., diabatic and adiabatic field ionization, of the same final Sr^{+*} state [11]. If we assume the right (higher field) peak results from ionization through the diabatic path and the left peak through the adiabatic path, the ratio of the threshold field strength of the diabatic ionization to that of the adiabatic ionization must be ≥ 1.8, not the experimental value of 1.5,

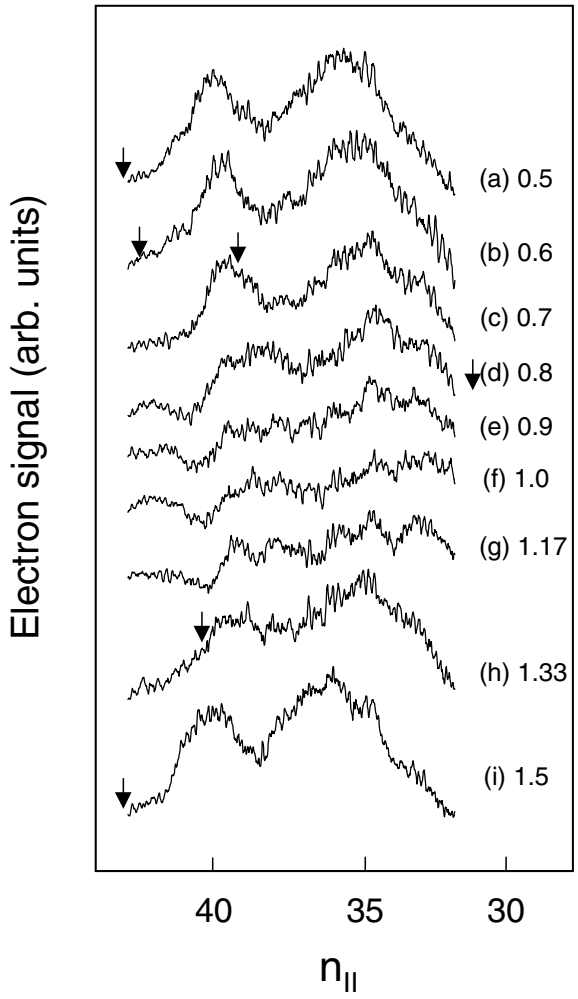

FIG. 4. Final-state distributions observed as an initial wave packet of $\bar{n} = 30.8$ evolves from the outer turning point (a) to the inner turning point (f), and to the outer turning point (i) again. The arrows show where the peaks should be if the outer electron is projected onto the Sr^{+*} final states. For (e) through (g) the arrow would be at too low a value of n_{II} to plot. In all traces, the background signal is subtracted from the observed signal.

however. A more interesting possibility has been suggested by Rosen *et al.* [6]. In their observations of IEI from high-l Sr $5fnl$ states they found the final values of n_{II} to be significantly lower than expected for a projection of the outer electron onto Sr^{+*} final states. They pointed out that, due to the long-range Coulomb interaction of the electrons, the inner electron cannot leave quickly compared to τ_K so that it is unlikely for the outer electron to be projected onto the Sr^{+*} final states. They also solved the time-dependent Schrödinger equation for a two-electron atom numerically. They found a double peaked Sr^{+*} final-state distribution very similar to the ones shown in Fig. 4 but displaced to a lower value of n_{II} than we have observed. It would be fascinating to repeat their calculations for a wave packet.

In conclusion, we have studied IEI from the radially localized $5snd$ Rydberg wave packet of Sr using a 200-fs laser pulse. As expected, IEI occurs only when the nd electron is far from the core. Measurements of the final Sr^{+*} state distribution show that the outer electron is not simply projected onto Sr^{+} Rydberg states in IEI. Rather, the two electrons interact during IEI to produce a double peaked final-state distribution.

We thank R. R. Jones for many useful discussions and experimental support on the fs-laser system. We also thank M. W. Noel for fruitful discussions. This work is supported by the U.S. Department of Energy.

[1] See, for example, L. F. DiMauro and P. Agostini, Adv. At. Mol. Opt. Phys. **35**, 79 (1995); M. Protopapas, C. H. Keitel, and P. L. Knight, Rep. Prog. Phys. **60**, 389 (1997).

[2] L. F. DiMauro, in *Many-Body Theory of Atomic Structure and Photoionization* (World Scientific, New Jersey, 1993), p. 297; D. N. Fittinghoff, P. R. Bolton, B. Chang, and K. C. Kulander, Phys. Rev. Lett. **69**, 2642 (1992); B. Walker, B. Sheehy, L. F. DiMauro, P. Agostini, K. J. Schafer, and K. C. Kulander, Phys. Rev. Lett. **73**, 1227 (1994).

[3] H. Stapelfeldt, D. G. Papaioannou, L. D. Noordam, and T. F. Gallagher, Phys. Rev. Lett. **67**, 3223 (1991).

[4] R. R. Jones and P. H. Bucksbaum, Phys. Rev. Lett. **67**, 3215 (1991).

[5] D. A. Tate and T. F. Gallagher, Phys. Rev. A **58**, 3058 (1998).

[6] C. Rosen, M. Dörr, U. Eichmann, and W. Sandner, Phys. Rev. Lett. **83**, 4514 (1999).

[7] J. Parker and C. R. Stroud, Jr., Phys. Rev. Lett. **56**, 716 (1986); G. Alber, H. Ritsch, and P. Zoller, Phys. Rev. A **34**, 1058 (1986); I. Sh. Averbukh and N. F. Perelman, Phys. Lett. A **139**, 449 (1989).

[8] L. D. Noordam, D. I. Duncan, and T. F. Gallagher, Phys. Rev. A **45**, 4734 (1992); R. R. Jones, C. S. Raman, D. W. Schumacher, and P. H. Bucksbaum, Phys. Rev. Lett. **71**, 2575 (1993).

[9] R. B. Vrijen and L. D. Noordam, J. Opt. Soc. Am. B **13**, 189 (1996).

[10] T. F. Gallagher, *Rydberg Atoms* (Cambridge University Press, Cambridge, England, 1994).

[11] J. H. M. Neijzen and A. Dönszelmann, J. Phys. B **15**, L87 (1982).